A Photopatternable Conjugated Polymer with Thermal-Annealing-Promoted Interchain Stacking for Highly Stable Anti-Counterfeiting Materials

Chengwei Liu, Ann-Kathrin Steppert, Yazhi Liu, Philipp Weis, Jianyu Hu, Chen Nie, Wen-Cong Xu, Alexander J. C. Kuehne,* and Si Wu*

Photoresponsive polymers can be conveniently used to fabricate anti-counterfeiting materials through photopatterning. However, an unsolved problem is that ambient light and heat can damage anti-counterfeiting patterns on photoresponsive polymers. Herein, photo- and thermostable anti-counterfeiting materials are developed by photopatterning and thermal annealing of a photoresponsive conjugated polymer (MC-Azo). MC-Azo contains alternating azobenzene and fluorene units in the polymer backbone. To prepare an anti-counterfeiting material, an MC-Azo film is irradiated with polarized blue light through a photomask, and then thermally annealed under the pressure of a photonic stamp. This strategy generates a highly secure anti-counterfeiting material with dual patterns, which is stable to sunlight and heat over 200 °C. A key for the stability is that thermal annealing promotes interchain stacking, which converts photoresponsive MC-Azo to a photostable material. Another key for the stability is that the conjugated structure endows MC-Azo with desirable thermal properties. This study shows that the design of photopatternable conjugated polymers with thermal-annealing-promoted interchain stacking provides a new strategy for the development of highly stable and secure anti-counterfeiting materials.

1. Introduction

Large amounts of anti-counterfeiting materials are needed for products, banknotes, medicines, and documents.[1–6] Photoresponsive polymers are promising candidates for the fast and easy fabrication of anti-counterfeiting patterns.[7–11] This is because patterns can be conveniently fabricated on photoresponsive polymers through a variety of photopatterning techniques, such as photolithography, laser direct writing, and two-photon absorption.[12–16] The irradiated regions of photoresponsive polymers change colors,[17–19] shapes,[20–27] solubilities,[28–30] or other properties,[31–33] and therefore exhibit contrasts compared to the nonirradiated regions. In this way, high-resolution quick response (QR) codes, logos, and other anti-counterfeiting patterns have been fabricated from photoresponsive polymers.[34–39] Such anti-counterfeiting patterns also exhibit user-defined functions and unclonable features, which have a high level of security.[7,40] Because of these advantages, many photoresponsive polymers have been developed for anti-counterfeiting in recent years.[7,35,41,42] However, an unsolved problem is that ambient light and heat can damage anti-counterfeiting patterns on photoresponsive polymers, which hinders their widespread and real-world application. For example, sunlight or even room light can damage anti-counterfeiting patterns on photoresponsive polymers because light induces further photoreactions. Additionally, anti-counterfeiting patterns on products may

C. Liu, Y. Liu, C. Nie, W.-C. Xu, S. Wu
CAS Key Laboratory of Soft Matter Chemistry
Anhui Key Laboratory of Optoelectronic Science and Technology
Department of Polymer Science and Engineering
University of Science and Technology of China
Hefei 230026, China
E-mail: siwu@ustc.edu.cn

A.-K. Steppert, A. J. C. Kuehne
Institute of Organic and Macromolecular Chemistry
Ulm University
Albert-Einstein-Allee 11, 89081 Ulm, Germany
E-mail: alexander.kuehne@uni-ulm.de

Y. Liu, P. Weis
Max Planck Institute for Polymer Research
Ackermannweg 10, 55128 Mainz, Germany

J. Hu
Department of Chemical Physics
School of Chemistry and Materials Science
University of Science and Technology of China
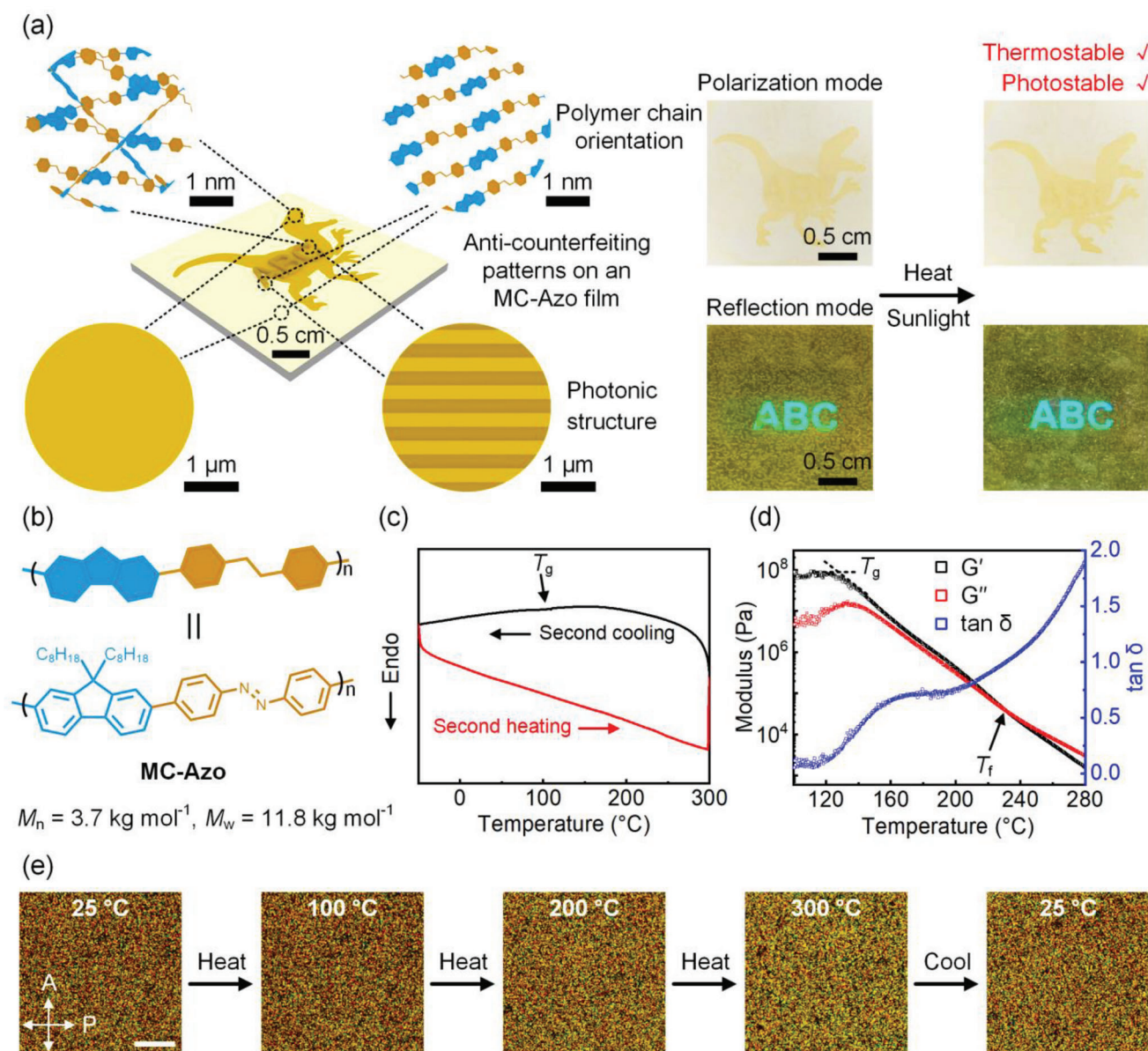Hefei 230026, China

Figure 1. a) Photostable and thermostable anti-counterfeiting patterns on an MC-Azo film. The polarized "dinosaur" pattern can be read out using polarized light, and the photonic "ABC" pattern can be read out with reflected light. The patterns are stable to sunlight and heat over 200 °C. b) Structure, number average molecular weight (M_n) and weight average molecular weight (M_w) of MC-Azo. c) Second heating and second cooling DSC curves of MC-Azo. d) Temperature dependence of rheology data of MC-Azo. G′: storage modulus; G″: loss modulus; tanδ = G″/G′: loss tangent. The glass transition temperature (T_g) determined using the decline in G′ is 127 °C. The flow temperature (T_f) determined by G″ = G′ is 231 °C. e) Polarized optical microscopy (POM) images of a drop-cast film of MC-Azo at different temperatures (thickness: ≈1.5 µm). The polarization directions for the crossed polarizers are P (polarizer) and A (analyzer). Scale bar: 25 µm.

experience high temperatures between 60 and 80 °C, for example, during transportation in the summer. Such temperatures can accelerate the motions of polymer chains or trigger back reactions of photoresponsive units, leading to the disappearance of anti-counterfeiting patterns.

Here, we develop photo- and thermostable anti-counterfeiting materials using a photoresponsive conjugated polymer (MC-Azo) (**Figure 1**a,b). MC-Azo contains alternating azobenzene and fluorene units in its backbone. On the one hand, azobenzene is a photoswitchable compound that shows reversible

cis-trans photoisomerization.[43-49] Furthermore, the orientation of azobenzene groups can be induced by polarized light that triggers *trans-cis-trans* cycling.[50-54] On the other hand, fluorene is an aromatic compound, which is a useful unit for the design of conjugated polymers with improved thermostability.[55,56] To prepare highly stable and secure anti-counterfeiting materials, an MC-Azo film was irradiated with polarized blue light through a photomask, and then thermally annealed under the pressure of a photonic stamp. An anti-counterfeiting material with highly secure dual patterns was obtained, which was stable

to sunlight and heat over 200 °C (Figure 1a). The stability is attributed to the desirable thermal properties of MC-Azo and thermal-annealing-promoted interchain stacking that converts photoresponsive MC-Azo into a photostable material. Our study opens up an avenue for the development of highly stable and secure anti-counterfeiting materials using photoresponsive conjugated polymers.

2. Results and Discussion

MC-Azo is a low-molecular-weight polymer that was synthesized via Suzuki-Miyaura polymerization (Figure 1b; Figures S1–S3, Supporting Information). The number average molecular weight (M_n), weight average molecular weight (M_w) and polydispersity index (PDI) of MC-Azo measured by gel permeation chromatography (GPC) were 3.7 kg mol^{-1}, 11.8 kg mol^{-1} and 3.2, respectively (Figure S4, Supporting Information). We also synthesized azopolymers with higher and lower molecular weights (MC-Azo-H and MC-Azo-L) and an azopolymer with two methyl groups as side chains (MC-Azo-methyl) as control samples (Figures S4 and S5, Supporting Information). MC-Azo had a decomposition temperature (T_d, 5% weight loss) of 370 °C, which showed that it exhibited high thermal stability (Figure S6, Supporting Information). The glass transition temperature (T_g) of MC-Azo measured by differential scanning calorimetry (DSC) was 109 °C (Figure 1c). Rheology measurements showed that MC-Azo exhibited a flow temperature (T_f) of 231 °C and a T_g of 127 °C, which is close to the DSC result (Figure 1d). Furthermore, a drop-cast film of MC-Azo exhibited anisotropic textures under polarized optical microscopy (POM) (Figure 1e). The textures were retained when the film was heated to 300 °C, suggesting that the clear point (T_c) of MC-Azo is higher than 300 °C. MC-Azo is a liquid crystal polymer because it is anisotropic above T_f. Moreover, the Young's modulus of MC-Azo measured by atomic force microscopy (AFM) was ≈2 GPa, which showed that it is a typical stiff conjugated polymer (Figure S7, Supporting Information). MC-Azo is fluorescent and has a quantum yield of 0.56 ± 0.16% (Figure S8, Supporting Information).

MC-Azo showed photoisomerization in solution (**Figure 2**a). Irradiating MC-Azo in tetrahydrofuran (THF) with 470 nm light induced *trans*-to-*cis* isomerization, while *cis*-to-*trans* back isomerization occurred thermally when the solution was kept in the dark at room temperature (Figure S9, Supporting Information). ^{1}H NMR spectra of MC-Azo in CDCl$_3$ before and after 470 nm light irradiation revealed that ≈22% *trans* isomers were converted to *cis* isomers, which was consistent with the UV–vis absorption data (Figure S10, Supporting Information).

To study the photoisomerization of MC-Azo in solid state, we prepared films by spin-coating (Figure 2b; Figure S11, Supporting Information). The MC-Azo film exhibited two absorption peaks at 419 and 296 nm, which were different from the characteristic absorption peaks of the individual azobenzene or fluorene unit (Figure 2c; Figure S12, Supporting Information). Density functional theory (DFT) simulations revealed that a new conjugated azobenzene-fluorene unit contributed to the natural transition orbital (NTO) levels (Figures S12–S14, Supporting Information). The absorption peaks at 419 and 296 nm were assigned to different transitions of the *trans* azobenzene-fluorene unit according to the DFT simulations (Figure S14, Supporting

Information). Under the irradiation of 470 nm light, the absorption peaks decreased, suggesting that *trans*-to-*cis* isomerization occurred (Figure 2c). The *cis* content at the photostationary state was 22% (Supporting Information). A higher *cis* content was not obtained because the absorption bands of the *trans* and *cis* isomers partially overlapped (Figure S13, Supporting Information). The *cis* isomer also absorbs blue light, which can induce *cis*-to-*trans* back isomerization. When the film in the photostationary state was kept in the dark at room temperature, *cis*-to-*trans* back isomerization occurred thermally (Figure S15, Supporting Information). Photoisomerization of MC-Azo-H and MC-Azo-L was also studied (Figure S16, Supporting Information). As the molecular weight increased, the degree of photoisomerization decreased. This result indicates that the mobility of the polymer chains decreased as the molecular weight increased. The result suggests that MC-Azo can be isomerized more easily than the high-molecular-weight sample MC-Azo-H. We studied MC-Azo after blue light illumination using POM and DSC. MC-Azo after illumination became slightly darker in POM, which agrees with the fact that illumination with blue light induced partial *trans*-to-*cis* isomerization. We infer that the slight change in POM is due to the relatively low *cis* content (21%) of MC-Azo at the photostationary state (Figure S17, Supporting Information). Moreover, no obvious T_g of MC-Azo after irradiation with blue light (21% *cis* content) was observed (Figure S18, Supporting Information).

Then, we annealed MC-Azo films at 200 °C for 12 h and studied the photoisomerization of the annealed films (Figure 2b3,b4). Upon vertical or oblique light irradiation (470 nm, 900 s, 15.3 mW cm^{-2}), the absorption spectra of annealed MC-Azo films were almost unchanged, which suggests that photoisomerization was turned off via thermal annealing (Figure 2d; Figure S19, Supporting Information). To elucidate the mechanism, we compared an MC-Azo film before and after annealing as well as MC-Azo in solution. After annealing, the absorption band of the MC-Azo film decreased significantly, and the maximum absorption wavelength shifted from 419 to 407 nm (Figure 2e). Compared with the MC-Azo solution and the MC-Azo film before annealing, the MC-Azo film exhibited a blueshifted absorption peak and broadened absorption band after annealing (Figure 2f). These results suggest that the chromophores formed more H- and J-aggregates in the annealed MC-Azo film (Figure 2b3). Additionally, the out-of-plane orientation of azobenzene chromophores also led to a decrease in absorption. UV–vis absorption spectra of an annealed MC-Azo film with different probe angles demonstrated that some MC-Azo polymers oriented perpendicular to the film plane (Figures S20 and S21, Supporting Information). The annealed MC-Azo is fluorescent (Figure S22, Supporting Information).

To further study the solid-state structures of MC-Azo, small-angle X-ray scattering (SAXS) and wide-angle X-ray scattering (WAXS) measurements were conducted. MC-Azo did not show any peaks in the SAXS profiles (Figure S23, Supporting Information). The 2D-WAXS pattern and WAXS profile of MC-Azo before annealing showed rings and peaks, revealing the presence of organized structures (Figure 2g,h). Peaks 1, 2 and 3 showed characteristic distances of 3.8, 4.6 and 5.5 Å, which were attributed to the interchain spacings. Peaks 2 and 2' were equally spaced in q-space (4.6 and 9.0 Å), indicating that they were attributed to different orders of WAXS signals. Peak 4 showed a characteristic
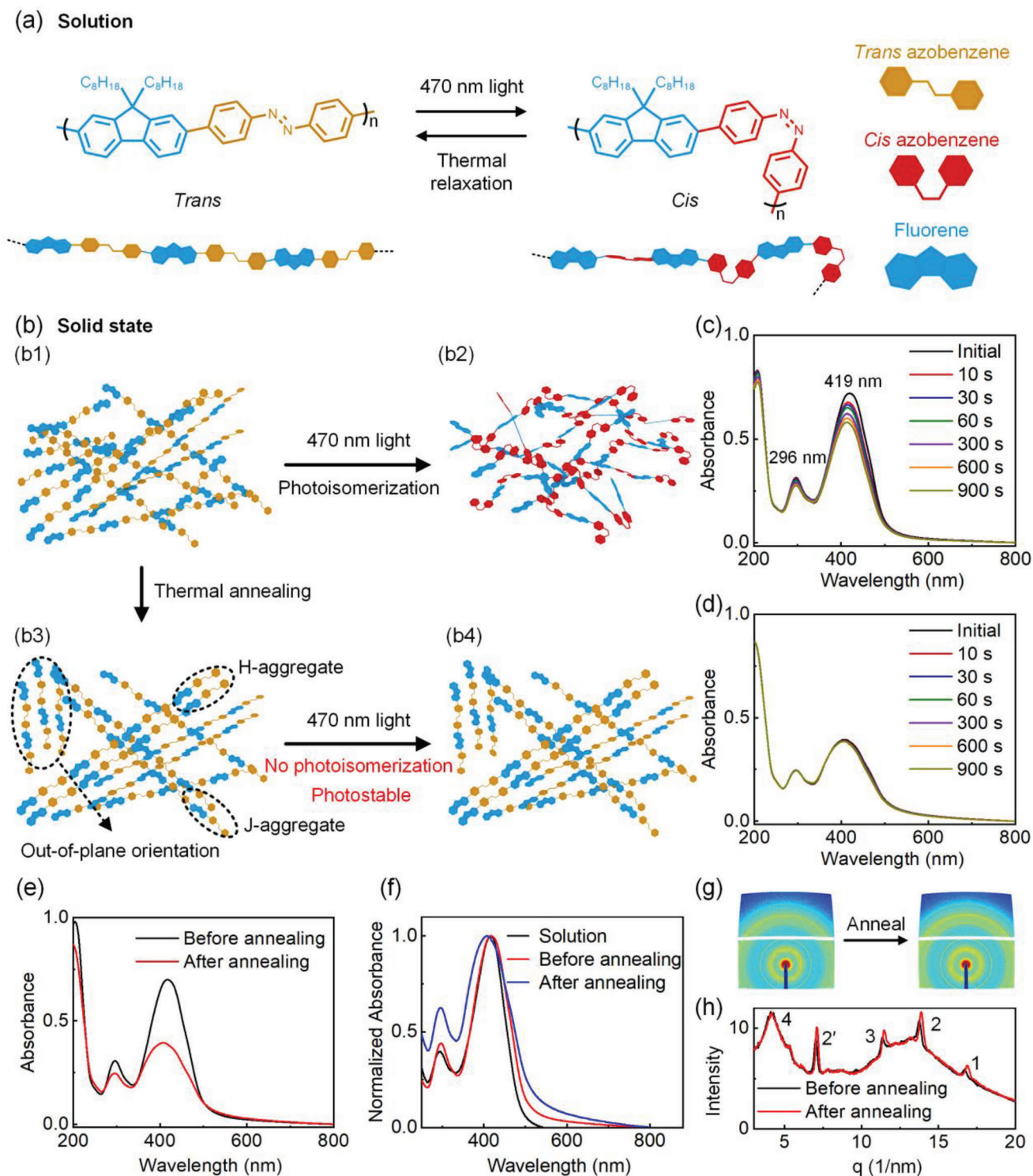
ADVANCED
SCIENCE NEWS
www.advancedsciencenews.com

ADVANCED
MATERIALS
www.advmat.de

Figure 2. a) *Cis-trans* isomerization of MC-Azo in solution. b) Effects of thermal annealing on photoisomerization of MC-Azo in solid state. Schematic of MC-Azo before (b1, b2) and after (b3, b4) thermal annealing upon 470 nm blue light irradiation. Thermal annealing promoted the formation of H- and J-aggregates, which turned off photoisomerization and made MC-Azo photostable. c,d) UV–vis absorption spectra of c) an unannealed and d) an annealed MC-Azo film (thickness: ≈69 nm) upon 470 nm light irradiation (15.3 mW cm^{-2}) for different time periods. e) UV–vis absorption spectra of an MC-Azo film (thickness: ≈69 nm) before and after thermal annealing at 200 °C for 12 h. f) Normalized UV–vis absorption spectra of a THF solution of MC-Azo and an MC-Azo film before and after annealing. g) 2D WAXS patterns and h) WAXS profiles of MC-Azo before and after annealing at 200 °C for 12 h.

2303120 (4 of 11)

ADVANCED
SCIENCE NEWS
www.advancedsciencenews.com

ADVANCED
MATERIALS
www.advmat.de

distance of 1.53 nm, which was similar to the length of a repeating unit of MC-Azo (Figure S24, Supporting Information). After MC-Azo was annealed at 200 °C for 12 h, the intensities and q values of all the peaks except for peak 4 increased, showing that the interchain structures became more ordered and close-packed. Peak 4 did not change after annealing, which indicated that the intrachain structure remained. Based on the WAXS and UV–vis absorption data, we interpret that photoisomerization of MC-Azo was turned off due to thermal-annealing-promoted interchain stacking, which enables the preparation of photostable anti-counterfeiting materials (see results below).

Next, we studied MC-Azo films under polarized blue light irradiation (**Figure 3**a). The polarized UV–vis absorption spectra of an unannealed MC-Azo film parallel and perpendicular to the polarizer of the spectrometer were identical, which shows that the film was macroscopically isotropic (Figure 3b). The film was then irradiated with linearly polarized light (470 nm, 15.3 mW cm^{-2}, 30 min). The absorption bands of the azobenzene-fluorene unit in the perpendicular direction were stronger than those in the parallel direction, which resulted in an order parameter of 0.13 (Figure 3c). It is well known that azobenzene chromophores can orient perpendicular to the polarization direction of linearly polarized light because of *trans-cis-trans* cycling.[51,57] This phenomenon is known as photoinduced orientation.[57,58] Our results showed that the azobenzene-fluorene units of MC-Azo orient perpendicular to the polarization direction of the polarized light. After irradiation with polarized blue light, the film was annealed at 200 °C for 12 h. Compared with the unannealed film, the annealed film had reduced, broadened, and blueshifted absorption bands and increased order parameters (Figure 3d). These results showed that interchain stacking was promoted by thermal annealing, enhancing the orientation. The birefringence of the MC-Azo film (≈520 nm) was studied (Figure S25, Supporting Information). After irradiation with linearly polarized light (470 nm, 15.3 mW cm^{-2}, 30 min), the birefringence of MC-Azo increased to 0.053 ± 0.002 and subsequently reached 0.083 ± 0.002 after annealing at 200 °C for 12 h. These results demonstrated that photoinduced birefringence and thermal-annealing-enhanced birefringence occurred.

Photoinduced orientation was also studied using polarized optical microscopy (POM). The dark POM images of an as-prepared MC-Azo film suggest that it was not aligned (Figure 3e). The film was irradiated with polarized light (470 nm, 15.3 mW cm^{-2}, 30 min, polarization direction 0°). The brightness of the film under POM varied with rotation of the sample and reached a maximum at a rotation angle of 45° (Figure 3f). This observation further corroborates the polarized light-induced orientation of MC-Azo. The film was then annealed at 200 °C for 12 h, where the POM signal became even brighter (Figure 3g). The result substantiates that thermal annealing promoted the orientation of the polymer chains.

In comparison, we studied the effects of thermal annealing on the photoinduced orientation using another MC-Azo film. The POM image showed that the as-prepared MC-Azo film was isotropic (Figure 3h). Upon annealing of the film at 200 °C for 12 h, some crystalline structures appeared (Figure 3i). Then, the annealed film was irradiated with polarized light (470 nm, 15.3 mW cm^{-2}, 30 min, polarization direction 0°), which was vertical or oblique to the film. The POM images were similar at dif-

ferent rotation angles, which showed that photoinduced orientation is not possible after thermal annealing (Figure 3j; Figure S26, Supporting Information). This experiment demonstrates again that thermal annealing can change photoresponsive MC-Azo to a photostable material. Additionally, annealed MC-Azo became photoresponsive when exposed to the vapor of a good solvent such as dichloromethane, while it retained photostable in the presence of the vapors of some solvents such as *n*-hexane and ethanol (Figure S27, Supporting Information).

Subsequently, we demonstrated photopatterning by irradiating an MC-Azo film with polarized light through a photomask (**Figure 4**a). A crab-shaped pattern was fabricated, which was observable under polarized light from a liquid crystal display (LCD) of a computer screen (Figure 4b). In contrast, the pattern was not visible under illumination by a lamp with unpolarized light. This polarization-dependent feature is promising for anti-counterfeiting. To showcase the applicability and multilevel security features, two patterns with different polarizations were prepared on the same film. To achieve this, an MC-Azo film was irradiated with polarized light (70°) through Mask 1, which is an array of circles, and then irradiated with polarized light (0°) through Mask 2, which consists of an array of squares (Figure 4c). The film showed different patterns under different rotation angles, which demonstrated the design of multilevel anti-counterfeiting patterns via polarization modulation. Meanwhile, we fabricated QR codes on MC-Azo films, which showed thermal-annealing-enhanced brightness under POM (Figure 4d,e).

Next, we investigated the stability of annealed polarized patterns of MC-Azo. An annealed QR-code pattern on an MC-Azo film was stable in a lab with ambient light at room temperature for 120 days, which revealed that the polarized pattern has long-term stability (Figure S28, Supporting Information). Considering that transported goods in shipping containers may experience temperatures as high as 60–80 °C, we tested whether polarized patterns of MC-Azo can be used as thermostable anti-counterfeiting materials. Our study showed that an annealed polarized pattern of MC-Azo was stable for 14 days at 80 °C (Figure 4f). Moreover, the annealed polarized pattern of MC-Azo was heated from 100 to 280 °C at intervals of 20 °C for one day at each temperature (Figure S29, Supporting Information). The pattern was stable up to temperatures of ≈200 °C. Only at 260 and 280 °C did the pattern show decreased brightness. These data suggest that the polarized patterns exhibit good thermal stability. We interpret that the thermal stability is in line with the high T_c and T_f of MC-Azo (Figure 1d,e).

We then studied the photostability of annealed polarized patterns of MC-Azo. An annealed polarized pattern was stable to solar lamp irradiation for 14 days (Figure 4g). Such an irradiance is identical to that of sunlight irradiance for 27 days in the southern Netherlands, 19 days in southern France and 14 days in Arizona, which demonstrated that annealed polarized patterns of MC-Azo exhibited photostability (Supporting Information). The polarized pattern was photostable because the photoresponsiveness of MC-Azo was turned off via thermal annealing.

We compared the stability of the polarized patterns on MC-Azo and several side-chain azopolymers with polynorbornene, polyacrylate, and polymethacrylate backbones. The comparison showed that the polarization patterns on the MC-Azo film were stable at 200 °C or under solar lamp irradiation for 14 days, while
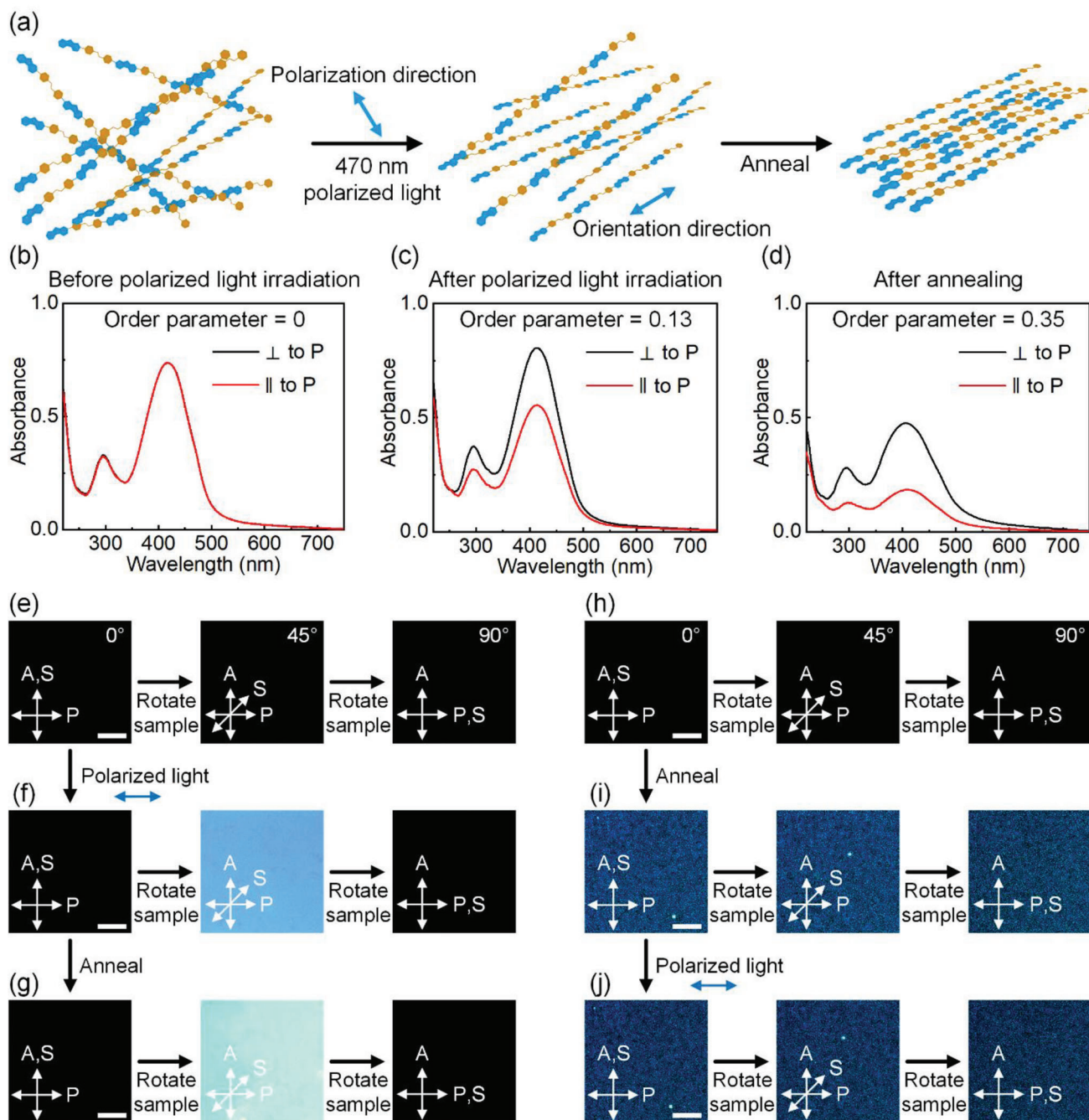
**ADVANCED
SCIENCE NEWS**

www.advancedsciencenews.com

**ADVANCED
MATERIALS**

www.advmat.de

Figure 3. a) Schematic of the photoinduced orientation and thermal-annealing-enhanced orientation of MC-Azo. b–d) Polarized UV–vis absorption spectra of an MC-Azo film (thickness: ≈69 nm) b) before polarized light irradiation, c) after polarized light irradiation (470 nm, 15.3 mW cm^{-2}, 30 min), and d) after subsequent annealing at 200 °C for 12 h. The direction of the polarizer in the spectrometer was parallel (red line) or perpendicular (black line) to the polarization direction of the 470 nm light. The order parameter, S, is determined by $S = (A_\perp - A_\parallel)/(A_\perp + 2A_\parallel)$, where $A_\parallel$ is the absorption at 419 nm in the parallel direction, and $A_\perp$ is the absorption at 419 nm in the perpendicular direction. e–g) POM images of an MC-Azo film (thickness: ≈69 nm) e) before irradiation, f) after polarized light irradiation (470 nm, 15.3 mW cm^{-2}, 30 min), and g) after subsequent annealing at 200 °C for 12 h. h–j) POM images of an MC-Azo film (thickness: ≈69 nm) h) before annealing, i) after annealing at 200 °C for 12 h, and j) after subsequent polarized light irradiation (470 nm, 15.3 mW cm^{-2}, 30 min). The polarization directions for the crossed polarizers are P (polarizer) and A (analyzer). The orientation directions of the MC-Azo films are S. The polarization direction of the 470 nm light is indicated by the double-headed blue arrows. Scale bars: 100 µm.
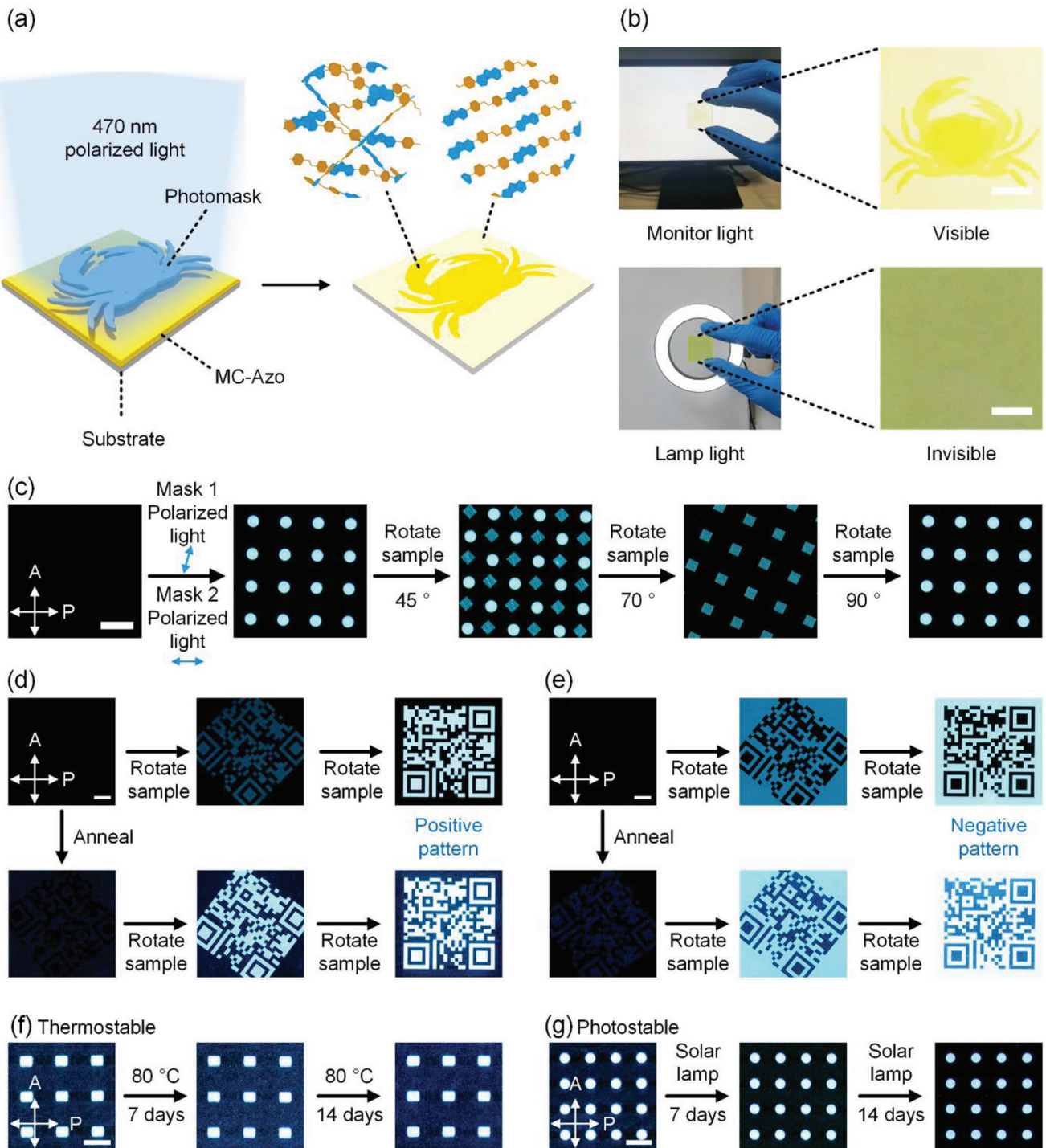
Figure 4. a) Schematic of the preparation of a polarized pattern. b) The polarized pattern was observable under monitor light and invisible under lamp light. Scale bars: 0.5 cm. c) POM images of two patterns with different polarizations on an MC-Azo film (thickness: ≈69 nm). Mask 1: an array of circles. Mask 2: an array of squares. Scale bar: 150 µm. d,e) POM images of QR codes on MC-Azo films (thickness: ≈69 nm) before and after annealing. Scale bar: 200 µm. f) POM images showing thermostability of a polarized pattern on an annealed MC-Azo film (thickness: ≈69 nm). Scale bar: 150 µm. g) POM images showing the photostability of a polarized pattern on an annealed MC-Azo film (thickness: ≈69 nm). The film was exposed to a solar lamp for 7 and 14 days. Scale bar: 150 µm. A: analyzer; P: polarizer.
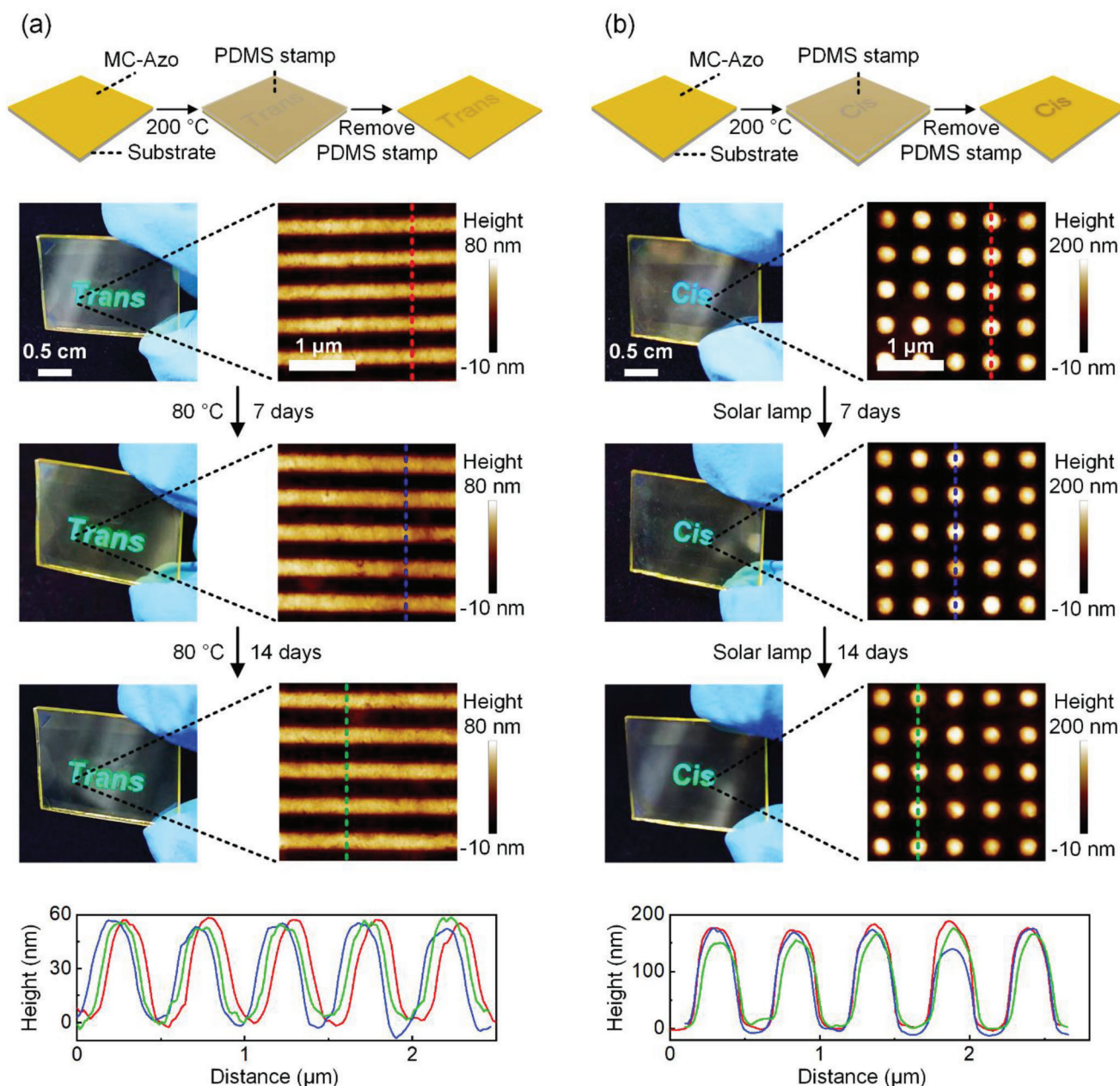
Figure 5. a) Preparation and thermostability of a photonic pattern on an MC-Azo film (thickness: ≈69 nm). The photonic pattern was imaged using AFM. The cross-sections are along the lines in the AFM images. b) Preparation and photostability of a photonic pattern on an MC-Azo film (thickness: ≈69 nm). The film was exposed to a solar lamp for 7 and 14 days. The irradiance of the solar lamp for 14 days is identical to sunlight irradiance for 27 days in the southern Netherlands, 19 days in southern France and 14 days in Arizona (Supporting Information). The cross-sections are along the lines in the AFM images.

the polarization patterns on the side-chain azopolymers were unstable at 80 °C or under solar lamp irradiation for 6 h (Figure S30, Supporting Information).

We noticed that thermal annealing can be combined with nanoimprinting to prepare photonic patterns on MC-Azo films (**Figure 5**). The photonic patterns "*Trans*" and "*Cis*" were prepared by annealing MC-Azo films at 200 °C for 12 h under the pressure of patterned polydimethylsiloxane (PDMS) stamps. The photonic patterns exhibited iridescent structural colors due

to their periodic structures (Figures S31 and S32, Supporting Information).

We tested the thermostability of the photonic patterns. Photographs and AFM images showed that the structural colors and nanostructures of the photonic pattern were almost unchanged after it was heated at 80 °C for 14 days (Figure 5a). Afterward, the photonic pattern was kept in a lab with ambient light at room temperature for 120 days (Figure S33, Supporting Information). It showed long-term stability. Furthermore, a photonic pattern of
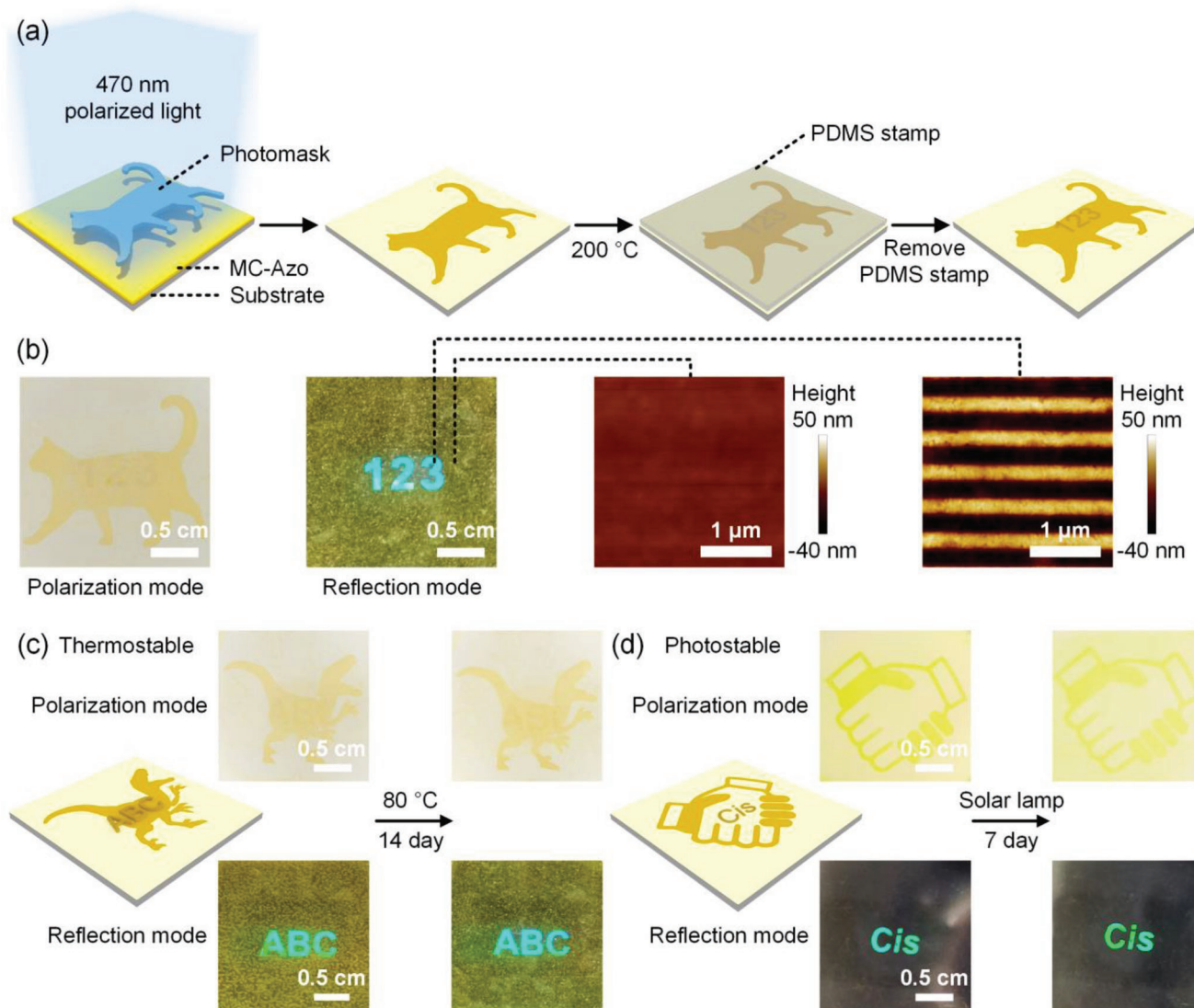
Figure 6. a) Schematic of the preparation of an anti-counterfeiting material that contains a cat-shaped polarized pattern and a 123-shaped photonic pattern. b) Dual patterns in the same MC-Azo film (thickness: ≈69 nm) observed under polarization and reflection modes. AFM images show the structures at different regions of the MC-Azo film. c) Thermostability of dual patterns of MC-Azo. After the MC-Azo film (thickness: ≈69 nm) was heated at 80 °C for 14 days, the dual patterns remained. d) Photostability of dual patterns of MC-Azo. The MC-Azo film (thickness: ≈69 nm) was irradiated with a solar lamp for 7 days. The irradiance is identical to sunlight irradiance for 13.5 days in the southern Netherlands, 9.5 days in southern France and 7 days in Arizona (Supporting Information).

MC-Azo was heated from 100 to 280 °C in 20 °C intervals for a day at each temperature (Figure S34, Supporting Information). The photonic pattern was stable up to 200 °C. Above 240 °C, the photonic pattern lost its integrity. We infer that the modest T_g of MC-Azo (109 °C) allows imprinting of photonic structures under pressure, while the high T_f of MC-Azo (231 °C) provides photonic structures with thermostability.

In addition, we tested the photostability of photonic patterns (Figure 5b). A photonic pattern was irradiated with a solar lamp for 14 days. The structural colors and nanostructures remained intact after irradiation, which demonstrated that the photonic pattern is photostable.

We also compared the thermo- and photostability of photonic patterns on MC-Azo with those on several side-chain azopolymers with polynorbornene, polyacrylate, and polymethacrylate backbones. The photonic patterns on the side-chain azopolymers were unstable at 80 °C or under solar lamp irradiation for 4 days, while the photonic patterns on MC-Azo were stable under these conditions (Figure S35, Supporting Information).

We further developed a procedure to combine a polarized pattern and a photonic pattern in an MC-Azo film, which can generate anti-counterfeiting materials with both high stability and improved security (**Figure 6**a). An MC-Azo film was irradiated with 470 nm of polarized light through a photomask, and then

2303120 (9 of 11)

**ADVANCED
SCIENCE NEWS**

www.advancedsciencenews.com

**ADVANCED
MATERIALS**

www.advmat.de

Figure 7. a) An inspection certificate for a car using anti-counterfeiting patterns of MC-Azo. b) Anti-counterfeiting labels of MC-Azo for products transported by containerization. Each package was labeled with an anti-counterfeiting label.

annealed at 200 °C under the pressure of a PDMS stamp. In this way, a cat-shaped polarized pattern and a 123-shaped photonic pattern were imposed on the same MC-Azo film (Figure 6b). The dual patterns were stable in a laboratory with ambient light and temperature for 60 days (Figure S36, Supporting Information). The two different patterns were also stable at 80 °C or under solar-lamp irradiation (Figure 6c,d).

Finally, we demonstrated that MC-Azo can be applied to daily use. For example, we fabricated an inspection certificate for a car (**Figure 7**a). The certificate can be observed from the window of the car. In addition, products transported by shipping containers also need highly stable and secure anti-counterfeiting labels because the transported goods that require anti-counterfeiting labels may experience high temperatures (60–80 °C) in the containers. We fabricated anti-counterfeiting patterns using MC-Azo for such products (Figure 7b; Movie S1, Supporting Information).

3. Conclusion

In conclusion, we have developed photo- and thermostable anti-counterfeiting materials by photopatterning and thermal annealing of a conjugated photoresponsive polymer MC-Azo. Its conjugated structure endowed MC-Azo with good thermostability, and interchain stacking promoted by thermal annealing enables switching of MC-Azo into a photostable state after photopatterning. Our study solves the intrinsic stability problem of photoresponsive polymers for anti-counterfeiting applications. The excellent stability combined with highly secure dual patterns makes MC-Azo a promising candidate for encryption, anti-counterfeiting, and information storage. We envision that the design of photopatternable conjugated polymers and thermal-

annealing-promoted interchain stacking reported here will pave the way for the development of photoresponsive materials with both new functions and high stability, both of which are important for practical applications.

4. Experimental Section

Detailed experimental procedures and characterizations are provided in the Supporting Information.

Statistical Analysis: The sample sizes for the measurements in Figures S8, S22, and S25 (Supporting Information) were 3. The absorption spectra in Figure 2f were normalized to [0,1]. The software used for statistical analysis was OriginPro 2020.

Supporting Information

Supporting Information is available from the Wiley Online Library or from the author.

Acknowledgements

2303120 (10 of 11)

**ADVANCED
SCIENCE NEWS**

www.advancedsciencenews.com

**ADVANCED
MATERIALS**

www.advmat.de

Conflict of Interest

The authors declare no conflict of interest.

Data Availability Statement

The data that support the findings of this study are available from the corresponding author upon reasonable request.

Keywords

[1] Y. Sun, X. Le, S. Zhou, T. Chen, *Adv. Mater.* **2022**, *34*, 2201262.
[2] J. B. Kim, C. Chae, S. H. Han, S. Y. Lee, S.-H. Kim, *Sci. Adv.* **2021**, *7*, eabj8780.
[3] J. H. Kim, G. H. Lee, J. B. Kim, S.-H. Kim, *Adv. Funct. Mater.* **2020**, *30*, 2001318.
[4] Z. Li, Y. Wang, G. Baryshnikov, S. Shen, M. Zhang, Q. Zou, H. Ågren, L. Zhu, *Nat. Commun.* **2021**, *12*, 908.
[5] T. Yimyai, T. Phakkeeree, D. Crespy, *Adv. Sci.* **2020**, *7*, 1903785.
[6] M. Li, Q. Lyu, B. Peng, X. Chen, L. Zhang, J. Zhu, *Adv. Mater.* **2022**, *34*, 2110488.
[7] W.-C. Xu, C. Liu, S. Liang, D. Zhang, Y. Liu, S. Wu, *Adv. Mater.* **2022**, *34*, 2202150.
[8] E. L. Prime, D. H. Solomon, *Angew. Chem., Int. Ed.* **2010**, *49*, 3726.
[9] Z. Pianowski, *Molecular Photoswitches: Chemistry, Properties, and Applications*, John Wiley & Sons, Hoboken, NJ, USA **2022**.
[10] Y. Yang, J. Wang, D. Li, J. Yang, M. Fang, Z. Li, *Adv. Mater.* **2021**, *33*, 2104002.
[11] K. Wang, J. Liu, P. Liu, D. Wang, T. Han, B. Tang, *J. Am. Chem. Soc.* **2023**, *145*, 4208.
[12] C. Probst, C. Meichner, K. Kreger, L. Kador, C. Neuber, H.-W. Schmidt, *Adv. Mater.* **2016**, *28*, 2624.
[13] H. S. Kang, J. C. Jolly, H. Cho, A. Kalpattu, X. A. Zhang, S. Yang, *Adv. Mater.* **2021**, *33*, 2005454.
[14] M. Regehly, Y. Garmshausen, M. Reuter, N. F. König, E. Israel, D. P. Kelly, C.-Y. Chou, K. Koch, B. Asfari, S. Hecht, *Nature* **2020**, *588*, 620.
[15] M. Gernhardt, V. X. Truong, C. Barner-Kowollik, *Adv. Mater.* **2022**, *34*, 2203474.
[16] L. García-Fernández, C. Herbivo, V. S. Arranz, D. Warther, L. Donato, A. Specht, A. del Campo, *Adv. Mater.* **2014**, *26*, 5012.
[17] X. Chen, W. Zhao, G. Baryshnikov, M. L. Steigerwald, J. Gu, Y. Zhou, H. Ågren, Q. Zou, W. Chen, L. Zhu, *Nat. Commun.* **2020**, *11*, 945.
[18] G. Weng, S. Thanneeru, J. He, *Adv. Mater.* **2018**, *30*, 1706526.
[19] Y. Liao, *Acc. Chem. Res.* **2017**, *50*, 1956.
[20] Z.-C. Jiang, Y.-Y. Xiao, X. Tong, Y. Zhao, *Angew. Chem., Int. Ed.* **2019**, *58*, 5332.
[21] M. P. da Cunha, M. G. Debije, A. P. H. J. Schenning, *Chem. Soc. Rev.* **2020**, *49*, 6568.
[22] M. Lahikainen, H. Zeng, A. Priimagi, *Nat. Commun.* **2018**, *9*, 4148.
[23] Y. Sun, M. Yang, Y. Guo, M. Cheng, B. Dong, F. Shi, *Angew. Chem., Int. Ed.* **2020**, *59*, 1098.
[24] A. H. Gelebart, D. J. Mulder, M. Varga, A. Konya, G. Vantomme, E. W. Meijer, R. L. B. Selinger, D. J. Broer, *Nature* **2017**, *546*, 632.
[25] J. Choi, W. Jo, S. Y. Lee, Y. S. Jung, S.-H. Kim, H.-T. Kim, *ACS Nano* **2017**, *11*, 7821.
[26] X. Zhao, Y. Chen, B. Peng, J. Wei, Y. Yu, *Angew. Chem., Int. Ed.* **2023**, *62*, 202300699.
[27] B. Peng, X. Chen, G. Yu, F. Xu, R. Yang, Z. Yu, J. Wei, G. Zhu, L. Qin, J. Zhang, Q. Shen, Y. Yu, *Adv. Funct. Mater.* **2023**, *33*, 2214172.
[28] J. L. Pelloth, P. A. Tran, A. Walther, A. S. Goldmann, H. Frisch, V. X. Truong, C. Barner-Kowollik, *Adv. Mater.* **2021**, *33*, 2102184.
[29] F. Seidi, Y. Zhong, H. Xiao, Y. Jin, D. Crespy, *Chem. Soc. Rev.* **2022**, *51*, 6652.
[30] S. Ludwanowski, O. Skarsetz, G. Creusen, D. Hoenders, P. Straub, A. Walther, *Angew. Chem., Int. Ed.* **2021**, *60*, 4358.
[31] R. Göstl, A. Senf, S. Hecht, *Chem. Soc. Rev.* **2014**, *43*, 1982.
[32] S. Yang, J. D. Harris, A. Lambai, L. L. Jeliazkov, G. Mohanty, H. Zeng, A. Priimagi, I. Aprahamian, *J. Am. Chem. Soc.* **2021**, *143*, 16348.
[33] L. Delafresnaye, F. Feist, J. P. Hooker, C. Barner-Kowollik, *Nat. Commun.* **2022**, *13*, 5132.
[34] Y. Liu, S. Liang, C. Yuan, A. Best, M. Kappl, K. Koynov, H.-J. Butt, S. Wu, *Adv. Funct. Mater.* **2021**, *31*, 2103908.
[35] B. Yang, F. Cai, S. Huang, H. Yu, *Angew. Chem., Int. Ed.* **2020**, *59*, 4035.
[36] H. Wang, H. K. Bisoyi, A. M. Urbas, T. J. Bunning, Q. Li, *J. Am. Chem. Soc.* **2019**, *141*, 8078.
[37] C. Hsu, Z. Xu, X. Wang, *Adv. Funct. Mater.* **2018**, *28*, 1802506.
[38] Y. Lim, B. Kang, S. J. Hong, H. Son, E. Im, J. Bang, S. Lee, *Adv. Funct. Mater.* **2021**, *31*, 2104105.
[39] D. Shen, Y. Yao, Q. Zhuang, S. Lin, *Macromolecules* **2021**, *54*, 10040.
[40] A. J. J. Kragt, D. C. Hoekstra, S. Stallinga, D. J. Broer, A. P. H. J. Schenning, *Adv. Mater.* **2019**, *31*, 1903120.
[41] A. Goulet-Hanssens, F. Eisenreich, S. Hecht, *Adv. Mater.* **2020**, *32*, 1905966.
[42] R. Klajn, *Chem. Soc. Rev.* **2014**, *43*, 148.
[43] A. Gonzalez, E. S. Kengmana, M. V. Fonseca, G. G. D. Han, *Mater. Today Adv.* **2020**, *6*, 100058.
[44] A. Gonzalez, M. Odaybat, M. Le, J. L. Greenfield, A. J. P. White, X. Li, M. J. Fuchter, G. G. D. Han, *J. Am. Chem. Soc.* **2022**, *144*, 19430.
[45] H. Zhou, C. Xue, P. Weis, Y. Suzuki, S. Huang, K. Koynov, G. K. Auernhammer, R. Berger, H.-J. Butt, S. Wu, *Nat. Chem.* **2017**, *9*, 145.
[46] W.-C. Xu, S. Sun, S. Wu, *Angew. Chem., Int. Ed.* **2019**, *58*, 9712.
[47] Z.-Y. Zhang, Y. He, Z. Wang, J. Xu, M. Xie, P. Tao, D. Ji, K. Moth-Poulsen, T. Li, *J. Am. Chem. Soc.* **2020**, *142*, 12256.
[48] M. A. Strauss, H. A. Wegner, *Angew. Chem., Int. Ed.* **2019**, *58*, 18552.
[49] J.-A. Lv, Y. Liu, J. Wei, E. Chen, L. Qin, Y. Yu, *Nature* **2016**, *537*, 179.
[50] Y. Wu, T. Ikeda, Q. Zhang, *Adv. Mater.* **1999**, *11*, 300.
[51] P. Karageorgiev, D. Neher, B. Schulz, B. Stiller, U. Pietsch, M. Giersig, L. Brehmer, *Nat. Mater.* **2005**, *4*, 699.
[52] D. Han, X. Tong, Y. Zhao, Y. Zhao, *Angew. Chem., Int. Ed.* **2010**, *49*, 9162.
[53] Y. Morikawa, S. Nagano, K. Watanabe, K. Kamata, T. Iyoda, T. Seki, *Adv. Mater.* **2006**, *18*, 883.
[54] K. G. Yager, C. J. Barrett, *Curr Opin Solid State Mater Sci* **2001**, *5*, 487.
[55] A. J. C. Kuehne, M. C. Gather, J. Sprakel, *Nat. Commun.* **2012**, *3*, 1088.
[56] V. H. K. Fell, A. Mikosch, A.-K. Steppert, W. Ogieglo, E. Senol, D. Canneson, M. Bayer, F. Schoenebeck, A. Greilich, A. J. C. Kuehne, *Macromolecules* **2017**, *50*, 2338.
[57] A. Natansohn, P. Rochon, *Chem. Rev.* **2002**, *102*, 4139.
[58] W. M. Gibbons, P. J. Shannon, S.-T. Sun, B. J. Swetlin, *Nature* **1991**, *351*, 49.